Precession, nutation, and space geodetic determination of the Earth's variable gravity field

G. Bourda, Nicole Capitaine

HAL Id: hal-00120000
https://hal.sorbonne-universite.fr/hal-00120000v2

Submitted on 30 Jun 2011

Astronomy
&
Astrophysics

Precession, nutation, and space geodetic determination of the Earth's variable gravity field

G. Bourda and N. Capitaine

Observatoire de Paris, SYRTE/UMR 8630-CNRS, 61 avenue de l'Observatoire, 75014 Paris, France
e-mail: bourda@syrte.obspm.fr; e-mail: capitaine@syrte.obspm.fr

Abstract. Precession and nutation of the Earth depend on the Earth's dynamical flattening, H, which is closely related to the second degree zonal coefficient, J_2 of the geopotential. A small secular decrease as well as seasonal variations of this coefficient have been detected by precise measurements of artificial satellites (Nerem et al. 1993; Cazenave et al. 1995) which have to be taken into account for modelling precession and nutation at a microarcsecond accuracy in order to be in agreement with the accuracy of current VLBI determinations of the Earth orientation parameters. However, the large uncertainties in the theoretical models for these J_2 variations (for example a recent change in the observed secular trend) is one of the most important causes of why the accuracy of the precession-nutation models is limited (Williams 1994; Capitaine et al. 2003). We have investigated in this paper how the use of the variations of J_2 observed by space geodetic techniques can influence the theoretical expressions for precession and nutation. We have used time series of J_2 obtained by the "Groupe de Recherches en Géodésie spatiale" (GRGS) from the precise orbit determination of several artificial satellites from 1985 to 2002 to evaluate the effect of the corresponding constant, secular and periodic parts of H and we have discussed the best way of taking the observed variations into account. We have concluded that, although a realistic estimation of the J_2 rate must rely not only on space geodetic observations over a limited period but also on other kinds of observations, the monitoring of periodic variations in J_2 could be used for predicting the effects on the periodic part of the precession-nutation motion.

Key words. astrometry – reference systems – ephemerides – celestial mechanics – standards

1. Introduction

Expressions for the precession of the equator rely on values for the precession rate in longitude that have been derived from astronomical observations (i.e. observations that were based upon optical astrometry until the IAU1976 precession, and then on Very Long Baseline Interferometry (VLBI) observations for more recent models). The IAU2000 precession-nutation model provided by Mathews et al. (2002) (denoted MHB 2000 in the following), that was adopted by the IAU beginning on 1 January 2003, includes a new nutation series for a non-rigid Earth and corrections to the precession rates in longitude and obliquity that were estimated from VLBI observations during a 20-year period. The precession in longitude for the equator being a function of the Earth's dynamical flattening H, observed values for this precession quantity are classically used to derive a realistic value for H. Such a global dynamical parameter of the Earth is generally considered as a constant, except in a few recent models for precession (Williams 1994; Capitaine et al. 2003) or nutation (Souchay & Folgueira 1999; Mathews et al. 2002; Lambert & Capitaine 2004) in which either the secular or the zonal variations of this coefficient are explicitly considered through simplified models.

The recent implementation of the IAU2000 A precession-nutation model guarantees an accuracy of about 200 μas in the nutation angles, and all the predictable effects that have amplitudes of the order of 10 μas have therefore to be considered. One of these effects is the influence of the variations (ΔH) in the Earth's dynamical flattening, which are not explicitly considered in the IAU2000 A precession-nutation model. Furthermore, the IAU2000 precession is based on an improvement of the precession rates values derived from recent VLBI measurements, but it does not improve the higher degree terms in the polynomials for the precession angles ψ_A, ω_A of the equator (see Fig. 1). This precession model is not dynamically consistent because the higher degree precession terms are actually dependent on the precession rates (Capitaine et al. 2003) and need to be improved, even though VLBI observations are unable to discriminate between recent solutions due to the limited span of the available data (Capitaine et al. 2004). One alternative way for such an improvement is to improve the model for the geophysical contributions to the precession angles and especially the influence of ΔH (or equivalently ΔJ_2).

The H parameter is linked to the dynamical form-factor, J_2 for the Earth (i.e. the C_{20} harmonic coefficient of the geopotential) which is determined by space geodetic techniques on a regular basis. Owing to the accuracy now reached
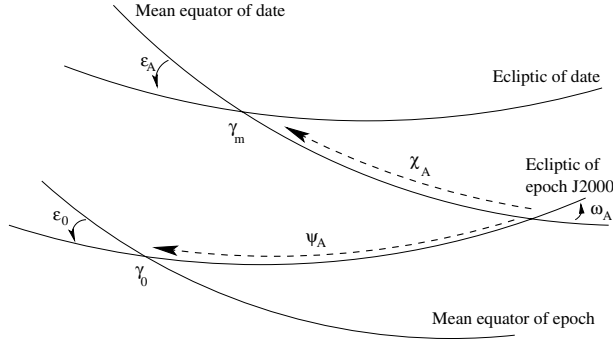
Fig. 1. Angles ψ_A and ω_A for the precession of the equator: γ_m is the mean equinox of the date and γ_0 is the equinox of the epoch J2000.0.

by these techniques, the temporal variation of a few Earth gravity field coefficients, especially ΔC_{20}, can be determined (for early studies, see for example Nerem et al. 1993; Cazenave et al. 1995; or Bianco et al. 1998). They are due to Earth oceanic and solid tides, as well as mass displacements of geophysical reservoirs and post-glacial rebound for ΔC_{20}. This coefficient C_{20} can be related to the Earth's orientation parameters and more particularly to the Earth precession-nutation, through H. The purpose of this paper is to use space geodetic determination of the geopotential to estimate ΔH, in order to investigate its influence on the precession-nutation model. The C_{20} data used in this study have been obtained from the positioning of several satellites between 1985 and 2002. We estimate also the constant part of H, based on such space geodetic measurements, and compare its value and influence on precession results with respect to those based on VLBI determinations.

In Sect. 2 we recall the equations expressing the equatorial precession angles as a function of the dynamical flattening H. We provide the numerical values implemented in our model, compare the values obtained for H by various studies and discuss the methods on which they rely. In Sect. 3 the relationship between ΔH and ΔC_{20} is discussed, depending on the method implemented. We explain how these geodetic data are taken into account in Sect. 4. We present our results in Sect. 5, and discuss them in the last part. We investigate how the use of a geodetic determination of the variable geopotential can influence the precession-nutation results, considering first the precession alone, and second the periodic contribution.

In the whole study, the time scale for t is TT Julian centuries since J2000, which will be denoted cy.

2. Theoretical effect of ΔH on precession

This section investigates the theoretical effect of the variations ΔH in the Earth's dynamical flattening on the precession expressions.

2.1. Relationship between H and the precession of the equator

The two basic angles ψ_A and ω_A (see Fig. 1) for the precession of the equator are provided by the following differential

equations (see Eq. (29) of Williams (1994) or Eq. (24) of Capitaine et al. (2003)):

$$\sin \omega_A \; \frac{d\psi_A}{dt} = \left(r_\psi \; \sin \epsilon_A\right) \; \cos \chi_A - r_\epsilon \; \sin \chi_A$$
$$\frac{d\omega_A}{dt} = r_\epsilon \; \cos \chi_A + \left(r_\psi \; \sin \epsilon_A\right) \; \sin \chi_A \tag{1}$$

where r_ψ and r_ϵ are respectively the precession rates in longitude and obliquity, ϵ_A is the obliquity of the ecliptic of date and χ_A the planetary precession angle, determining the precession of the ecliptic. Updated expressions for these precession quantities are given in Capitaine et al. (2003). An expression for the precession rates, r_ψ in longitude and r_ϵ in obliquity, is provided in detail in Williams (1994) and Capitaine et al. (2003) as a function of various contributions. The precession rate in longitude can be written as $r_\psi = r_0 + r_1 \, t + r_2 \, t^2 + r_3 \, t^3$ where the largest first-order term in r_0 is the luni-solar contribution denoted $f_{01_{|LS}} \cos \epsilon_0$, where ϵ_0 is the obliquity of the ecliptic at J2000. It is such that (Kinoshita 1977; Dehant & Capitaine 1997):

$$f_{01_{|LS}} = k_m \, M_0 + k_s \, S_0 \tag{2}$$

in which M_0 and S_0 are the amplitudes of the zero-frequency Moon and Sun attractions, respectively, and:

$$k_m = 3 H \frac{m_m}{m_m + m_\oplus} \frac{1}{F_2{}^3} \frac{n_m^2}{\Omega} = H \, K_m \tag{3}$$

$$k_s = 3 H \frac{m_\odot}{m_\odot + m_m + m_\oplus} \frac{n_\odot^2}{\Omega} = H \, K_s. \tag{4}$$

In the above expressions, H is the Earth's dynamical flattening, m_m, $m_\odot$ and $m_\oplus$ are the masses of the Moon, the Earth and the Sun, respectively, n_m is the Moon mean motion around the Earth, $n_\odot$ the Earth mean motion around the Sun, Ω is the mean angular velocity of the Earth and F_2 a factor for the mean distance of the Moon. Current numerical values for such a problem are (Souchay & Kinoshita 1996):

$$M_0 = 496\,303.66 \times 10^{-6}$$
$$S_0 = 500\,210.62 \times 10^{-6}$$
$$k_m = 7546\rlap{.}{''}7173289 \,/cy \tag{5}$$
$$k_s = 3475\rlap{.}{''}1883295 \,/cy$$
$$f_{01_{|LS}} \cos \epsilon_0 = 5040\rlap{.}{''}6445 \,/cy$$

and (see Kinoshita 1977):

$$F_2 = 0.999093142.$$

Hence, the link between the precession of the equator (ψ_A and ω_A angles) and the Earth's dynamical flattening (H) is shown by Eqs. (1)−(4) and (7) of Sect. 2.2. Classically, H is related to $f_{01_{|LS}}$ derived from observations by:

$$H = \frac{f_{01_{|LS}}}{K_m \, M_0 + K_s \, S_0}. \tag{6}$$

Table 1. Comparison between constants used for different determinations of the dynamical flattening (H): (1) the precession rate in longitude (ψ_1); (2) the speed of the general precession in longitude (p_1); (3) the geodesic precession (p_g); and (4) the obliquity of the ecliptic at J2000.0 (ϵ_0). The observational value actually used for each study is written in bold.

Sources	H ($\times 10^3$)	(1) ψ_1	(2) p_1	(3) p_g	(4) ϵ_0
		(in ''/cy)			
Lieske et al. (1977)		5038.7784	**5029.0966**	−1.92	23°26′21″.448
Kinoshita (1977) and Seidelmann (1982)	3.2739935	5038.7784	**5029.0966**	−1.92	23°26′21″.448
Williams (1994)	3.2737634	**5038.456501**	5028.7700	−1.9194	23°26′21″.409
Souchay & Kinoshita (1996)	3.2737548	–	5028.7700	−1.9194	23°26′21″.448
Bretagnon et al. (1997)	3.2737671	5038.456488	**5028.7700**	−1.919883	23°26′21″.412
Bretagnon et al. (2003)	–	5038.478750	**5028.792262**	−1.919883	23°26′21″.40880
Fukushima (2003)	3.2737804	**5038.478143**	5028.7955	−1.9196	23°26′21″.40955
Capitaine et al. (2003)	3.27379448	**5038.481507**	5028.796195	−1.919883	23°26′21″.406
Mathews et al. (2002)	3.27379492	**5038.478750**	5028.7923	−1.9198	23°26′21″.410

2.2. Astronomical determination of H

We can write r_0 as:

$$r_0 = f_{01|_{LS}} \cos \epsilon_0 + f_{01|_{PL}} \cos \epsilon_0 \qquad (7)$$
$$+ H \times \text{lunisolar second order effects}$$
$$+ H \times (J_2 \text{ and planetary}) \text{ tilt effects}$$
$$+ J_4 \text{ lunisolar effect}$$
$$- \text{geodesic precession}$$
$$+ \text{non-linear effects (Mathews et al. 2002)}$$

where $f_{01|_{PL}}$ is the first order term of the planetary contribution (also proportional to H). Classically, H is derived from observationally determined values of r_0. The measurement of r_0 should be corrected by removing the modelled contributions other than the lunisolar first order effect (see Eq. (7)). Hence, we obtain a value for $f_{01|_{LS}}$, which is the only term with sufficiently large amplitude (of the order of $5000''$/cy) to be sensitive to small changes in the value of the dynamical ellipticity H of the Earth (see Eq. (6)). So, given the other contributions provided by the theory, we can derive the value of H from the observed value of r_0 and the model for the lunisolar first order effects.

A major problem consists in choosing the constant value of H. Indeed, depending on the authors, it differs by about 10^{-7} (Table 1). This is due to the different measurements and models implemented (see Fig. 1 of Dehant & Capitaine 1997; Fig. 5 of Dehant et al. 1999). On the one hand the optical measurements give values of the general precession in longitude p_A referred to the ecliptic of date, whereas VLBI gives measurements relative to space. On the other hand, the various constants and models used for obtaining the value for H from a measured value (optical, Lunar laser ranging or VLBI) are different depending on the study considered (see Eq. (7)).

Classically, ψ_A is developed in a polynomial form of t as: $\psi_A = \psi_0 + \psi_1 t + \psi_2 t^2 + \psi_3 t^3$. In Table 1, we recall the different values used (i) for ψ_1 (i.e. the precession rate in longitude, $\psi_1 = r_0$), directly obtained from VLBI measurements,

and (ii) for p_1 which is the observationally determined value of precession in the optical case: $\psi_1 = p_1 + \chi_1 \cos \epsilon_0$ (Lieske et al. 1977).

The computation of the IAU2000 precession-nutation model by Mathews et al. (2002) is based on a new method which uses geophysical considerations. They adjust nine Basic Earth Parameters (BEP), including the Earth dynamical flattening H.

2.3. Method and parameters used in this study

Based on the paper by Capitaine et al. (2003), denoted hereafter P03, we use differential Eq. (1) in which H has been replaced by $H + \Delta H$ (using Eqs. (2)−(4) and (7)). We start from the P03 initial values for the variables ω_A, ψ_A, ϵ_A, χ_A and p_A, that are represented as polynomials of time and rely on the numerical values given in Table 2. We solve Eq. (1) together with the other precession equations (e.g. see Eqs. (26) and (28) of P03) with the software GREGOIRE (Chapront 2003) that can process Fourier and Poisson expressions. We iterate this process until we obtain a convergence of the solution.

3. Relationship between C_{20} and H

3.1. Relation

From the geodetic C_{20} variation series we can derive the corresponding variations of the dynamical flattening H. Indeed, knowing that $J_2 = -C_{20} = -\sqrt{5}\, \bar{C}_{20}$, in the case of a rigid Earth, we can write (see Lambeck 1988):

$$H = \left(C - \frac{A+B}{2}\right)/C = \frac{M R_e^2}{C} J_2 \qquad (8)$$
$$= -\frac{M R_e^2}{C} C_{20}$$
$$= -\sqrt{5}\, \frac{M R_e^2}{C} \bar{C}_{20}$$

Table 2. Numerical values used in this study. H, ψ_1 and ω_1 are integration constants.

Initial values at J2000.0	
H	$H_{\mathrm{MHB}} = 3.27379492 \times 10^{-3}$
ψ_1	$5038.''481507$/cy
ω_1	$-0.''02575$/cy
p_1	$5028.''796195$/cy
χ_1	$10.''556403$/cy
ϵ_0	$84\,381.''406 = 23°26'21.''406$

Contributions to the precession rate in longitude (in $''$/cy)	
Lunisolar first order	$5494.062986 \times \cos\epsilon_0 \simeq 5040.7047$
Planetary first order	0.031
Geodesic precession	-1.919882

where A, B and C are the mean equatorial and polar moments of inertia of the Earth. M and R_e are respectively the mass and the mean equatorial radius of the Earth. $\bar{C}_{20}$ is the normalized Stokes coefficient (of degree 2 and order 0) of the geopotential.

But the Earth is elastic, so let us consider small variations of H, C_{20} and the third principal moment of inertia of the Earth (C being its constant part and c_{33} its variable part). Then we obtain:

$$H_{\text{total}} = \frac{M\,R_e^2}{C}\;\frac{1}{1+\frac{c_{33}}{C}}\;J_{2\,\text{total}} \tag{9}$$

c_{33}/C being a small quantity of the order of 10^{-6}, we consider the Taylor development of $(1 + c_{33}/C)^{-1}$. Then the total expression of H can be written as:

$$H_{\text{total}} = \frac{MR_e^2}{C}\,J_{2\,\text{total}}\left(1 - \frac{c_{33}}{C} + \left(\frac{c_{33}}{C}\right)^2 + ...\right) \tag{10}$$

where $MR_e^2/C \times (c_{33}/C)^n\,J_2$ for $n \geq 1$ is smaller than 10^{-11}. So, in Eq. (10), considering (i) constant and variable parts separately; and (ii) Eq. (8), we obtain:

$$\Delta H = \frac{MR_e^2}{C}\,\Delta J_2 = -\sqrt{5}\,\frac{MR_e^2}{C}\,\Delta\bar{C}_{20} \tag{11}$$

where $\Delta J_2 = -\Delta C_{20} = -\sqrt{5}\,\Delta\bar{C}_{20}$ corresponds to the variations of the Stokes coefficient J_2. Generally, we can write: $\Delta J_2 \propto c_{33}/C$ (Lambeck 1988).

3.2. Computation of the ratio MR_e^2/C

The coefficient MR_e^2/C is usually obtained from the H and J_2 values (see Eq. (8)). In order to determine the constant part of H, we can use (i) the R_e, M and C values; or (ii) the Clairaut theory (see Table 3).

First, recall the Earth geometrical flattening ϵ:

$$\epsilon = \frac{R_e - R_p}{R_e} \tag{12}$$

where R_p and R_e are respectively the polar and equatorial mean radii of the Earth. Second, recall the assumptions that the Earth (i) is in hydrostatic equilibrium; and (ii) is considered as a revolutional ellipsoid. Hence, the first Clairaut equation gives the Earth geometrical flattening as a function of J_2 and q. The approximations to the first and second order are respectively:

$$\epsilon = \frac{q}{2} + \frac{3}{2}J_2 \tag{13}$$

$$\epsilon = \frac{q}{2} + \frac{3}{2}J_2 + \frac{9}{8}J_2^2 - \frac{3}{14}J_2\,q - \frac{11}{56}q^2 \tag{14}$$

where the geodynamical constant is:

$$q = \frac{\omega^2 R_e^3}{GM} \tag{15}$$
$$= 3.461391 \times 10^{-3}, \quad \text{IAG (Groten 1999)}.$$

Then, the following Radau equation can help us to determine the expression of MR_e^2/C:

$$\frac{\epsilon - q/2}{H} = 1 - \frac{2}{5}\,\sqrt{1+\eta} = \frac{1}{\lambda} \tag{16}$$

where λ is the d'Alembert parameter and η the Radau parameter, as:

$$\eta = \frac{5q}{2\epsilon} - 2. \tag{17}$$

Hence, replacing ϵ with Eq. (13) in Eq. (16) and using Eq. (8) gives the Darwin-Radau relation as following:

$$\frac{C}{MR_e^2} = \frac{2}{3\lambda} = \frac{2}{3}\left(1 - \frac{2}{5}\,\sqrt{1+\eta}\right). \tag{18}$$

Our tests have shown that Eq. (14) for ϵ, in the expression (17) of η, gives more reliable results.

In Table 3 we compare the various H values obtained. We denote (i) H^* the value obtained with the Clairaut method and (ii) H^{**} the value obtained using directly the R_e, C and M values. Both are computed with Eq. (8) and a value for J_2 of 1.0826358×10^{-3}. Note that in contrast, IAG or MHB values (usually used) are determined from astronomical precession observations and can be used to compute the C/MR_e^2 value. We can add that the differences with H_{MHB} come from (i) the hydrostatic equilibrium hypothesis in Clairaut's theory for the value H^*; and (ii) the poorly determined R_e, C and M values, for the value H^{**}. This will introduce errors in the ΔH determination, which we will study in Sect. 3.3.

In the following, we will use the $C/\left(MR_e^2\right)$ value determined with the Clairaut theory, noted with a (*) in Table 3, which corresponds to a value for H of: $H^* = 3.26715240 \times 10^{-3}$.

3.3. Error estimation

We can estimate the error that the use of the Clairaut theory introduces into the ΔH results. Indeed, if we consider the MHB value as the realistic H value (see Table 3), the relative error made is:

$$\sigma_H = \frac{H_{\mathrm{MHB}} - H^*}{H_{\mathrm{MHB}}} \simeq 2 \times 10^{-3}. \tag{19}$$

Table 3. Comparison between different values of the coefficient $C/(MR_e^2)$ and of the constant part for H: (1) IAG values (Groten 1999) – (2) MHB values (Mathews et al. 2002) – (3) Constant part H^{**} obtained from Eq. (8) using the M, R_e and C IAG values – (4) Method of "Clairaut" (Sect. 3.2), assuming hydrostatic equilibrium. The third and fourth methods use a constant part for $\bar{C}_{20}$ of -4.841695×10^{-4} in Eq. (8) (i.e. $J_2 = 1.0826358 \times 10^{-3}$). The sense of the computation is indicated by the arrows.

	(1) IAG (1999)	(2) MHB 2000	(3) Separate values for M, R_e and C	(4) Clairaut Theory
$C/(MR_e^2)$	0.330701 $\pm 2 \times 10^{-6}$	0.330698	0.330722^{**}	0.331370^*
	$\Uparrow$	$\Uparrow$	$\Downarrow$	$\Downarrow$
H	3.273763×10^{-3} $\pm 2 \times 10^{-8}$	$3.27379492 \times 10^{-3}$	$H^{**} = 3.27355562 \times 10^{-3}$	$H^* = 3.26715240 \times 10^{-3}$

We estimate that the error is about 0.2%. So, computing the variable part of H with the C_{20} data results in a maximum error of about:

$$|\Delta H_{\text{real}} - \Delta H^*| \simeq \left(2 \times 10^{-3}\right) \times \left(6 \times 10^{-9}\right)$$
$$\simeq 1.2 \times 10^{-11} \tag{20}$$

assuming that the maximum value for ΔH is of the order of 6×10^{-9}. Then, regarding the values of the ΔH data and of their precision, we can consider this error as negligible.

4. Time series of ΔC_{20} used in this study

The geodetic data used are the time series (variable part) of the spherical harmonic coefficient C_{20} of the geopotential, obtained by the GRGS (Groupe de Recherche en Géodésie Spatiale, Toulouse) from the precise orbit determination of several satellites (like LAGEOS, Starlette or CHAMP) from 1985 to 2002 (Biancale et al. 2002). The combination of these satellites allows the separation of the different zonal geopotential coefficients, more particularly of J_2 and J_4. This series includes (i) a model part for the atmospheric mass redistributions (Chao & Au 1991; Gegout & Cazenave 1993) and for the oceanic and solid Earth tides (McCarthy 1996); and (ii) a residual part (see Fig. 2) obtained as difference of the space measurements with respect to a model. These various changes in the Earth system are modelled as variations in the standard geopotential coefficient C_{20} and we note the different contributions $\Delta C_{20_{\text{atm}}}$, $\Delta C_{20_{\text{oc}}}$, $\Delta C_{20_{\text{soltid}}}$ and $\Delta C_{20_{\text{res}}}$, respectively.

### 4.1. ΔC_{20} residuals and its secular trend: Observed part

Earlier studies already took into account the effect of the secular variation of C_{20} on the precession of the equator. Such a secular variation is attributed to the post-glacial rebound of the Earth (Yoder et al. 1983), which reduces its flattening. Williams (1994) and Capitaine et al. (2003) considered a J_2 rate value of -3×10^{-9}/cy. Using the numerical value of Table 2 for the first order contribution ($f_{01} \cos \epsilon_0$) to the precession rate r_0, which is directly proportional to J_2, the contribution $\dot{J}_2/J_2 \times f_{01} \cos \epsilon_0$ of the J_2 rate to the acceleration of precession $d^2\psi_A/dt^2$ is about $-0.014''/\text{cy}^2$, giving rise to
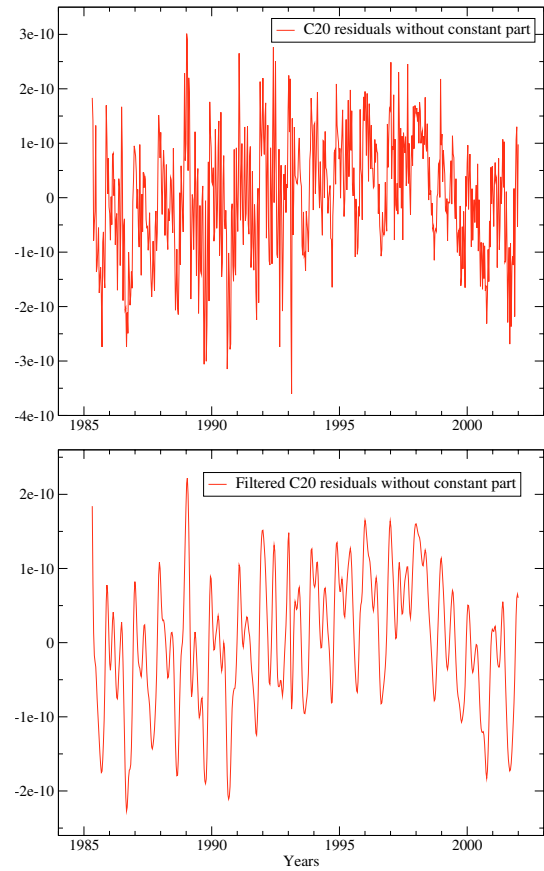
Fig. 2. Normalized ΔC_{20} residuals (*top*: raw residuals, *bottom*: filtered residuals, where the high frequency signals have been removed): non-modelled part of the ΔC_{20} harmonic coefficient of the Earth gravity field.

a $-0.007''/\text{cy}^2$ contribution to the t^2 term in the expression of ψ_A.

Since 1998, a change in the secular trend of the J_2 data has been reported (Cox & Chao 2000). This change can be seen in the series of $\Delta \bar{C}_{20}$ residuals (see Fig. 2). An attempt to model this effect, with oceanic data, water coverage data and geophysical models, has been investigated by Dickey et al. (2002). Using the residuals $\Delta \bar{C}_{20}$ of the GRGS, we can estimate a secular trend for $J_2 = -\sqrt{5}\,\bar{C}_{20}$ from 1985 to 1998 (see Fig. 3). We find a J_2 rate of the order of: $-2.5\,(\pm 0.2) \times 10^{-9}$/cy, which gives
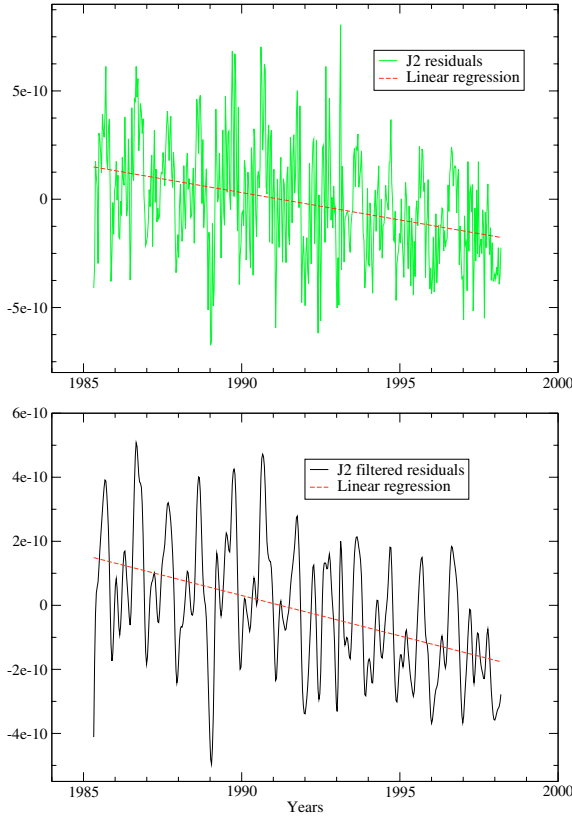
Fig. 3. J_2 GRGS residuals (*top*: raw residuals, *bottom*: filtered residuals, where the high frequency signals have been removed): estimation of the linear trend, from 1985 to 1998.

Fig. 4. Normalized atmospheric ΔC_{20} (*top*: raw data, *bottom*: filtered data, where the high frequency signals have been removed): atmospheric modelled part of the ΔC_{20} harmonic coefficient of the Earth gravity field, obtained with ECMWF pressure data.

a change of about $-0.006''/\text{cy}^2$ in the t^2 term of the polynomial development of the precession angle ψ_A.
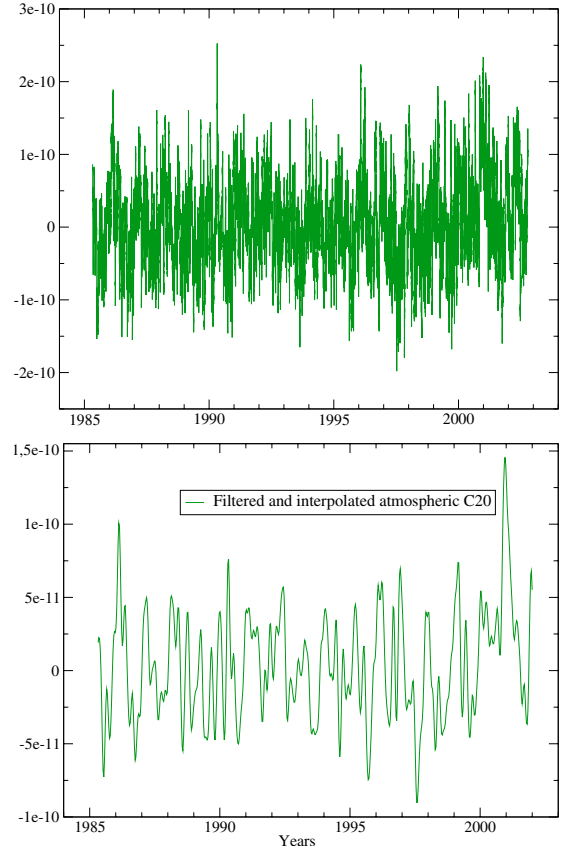
As this secular trend is not the same in the total data span, we will also model the long term variations in the C_{20} residual series with a periodic signal. Such a long-period term in the J_2 residual series may come from mismodelled effects, particularly from the 18.6-yr solid Earth tides. We will make such an assumption and adjust for the period 1985–2002, a secular trend and a long-period term in the ΔC_{20} residual series (see Sect. 4.3).

However, it should be noted that a secular trend for J_2, of the order of $-3 \times 10^{-9}/\text{cy}$, is more consistent with long term studies of the Earth rotation variations by Morrison & Stephenson (1997), based upon eclipse data over two millennia (they found $\dot{J}_2 = (-3.4 \pm 0.6) \times 10^{-9}/\text{cy}$).

4.2. ΔC_{20} geophysical data used: Modelled part

The geophysical models that have been previously subtracted from the C_{20} data (i.e. atmospheric, oceanic and solid Earth tides effects) must be added back to these data in exactly the same way they had been subtracted to reconstruct the relevant geophysical contributions.

For each contribution we give the associated potential U at the point (r, ϕ, λ, t) (limited to the degree 2 and order 0) that we identify with the Earth gravitational potential. Hence, we

obtain the $\Delta \bar{C}_{20}$ coefficient contribution of each geophysical source.

- The atmospheric contribution is due to pressure changes in time, measured and given by the European Centre for Medium-range Weather Forecasts (ECMWF) (see Fig. 4). The simple-layer atmospheric potential, limited to degree 2 and order 0, can be expressed as:

$$U_{\text{atm}} = 4\pi G R_{\text{e}} \frac{1 + k'_2}{5g} \left(\frac{R_{\text{e}}}{r}\right)^3 \Delta \bar{C}_{20_{\text{ECMWF}}}(t) \, \bar{P}_{20}(\sin \phi) \quad (21)$$

where $G = 6.672 \times 10^{-11} \text{ m}^3 \text{ kg}^{-1} \text{ s}^{-2}$ is the gravitational constant, $k'_2 = -0.314166$ is a Love number (Farrell 1972), $g = 9.81 \text{ m s}^{-2}$, and $\bar{P}_{20}(\sin \phi)$ is the Legendre function of degree 2 and order 0. The $\bar{C}_{20_{\text{ECMWF}}}(t)$ atmospheric coefficient, expressed in Pascals, comes from the spherical harmonic decomposition of the ECMWF atmospheric pressure grids, every 6 h, over continents (see Gegout & Cazenave 1993; or Chao & Au 1991):

$$\Delta \bar{C}_{20_{\text{ECMWF}}}(t) = \int_S \Delta p \, (\phi, \lambda, t) \left(\frac{3}{2} \sin^2 \phi - \frac{1}{2}\right) \text{d}S \quad (22)$$

where S is a surface grid pressure around the Earth and Δp is the difference of pressure with a constant part prefixed, at the point (ϕ, λ). Hence, identifying Eq. (21) with the Earth
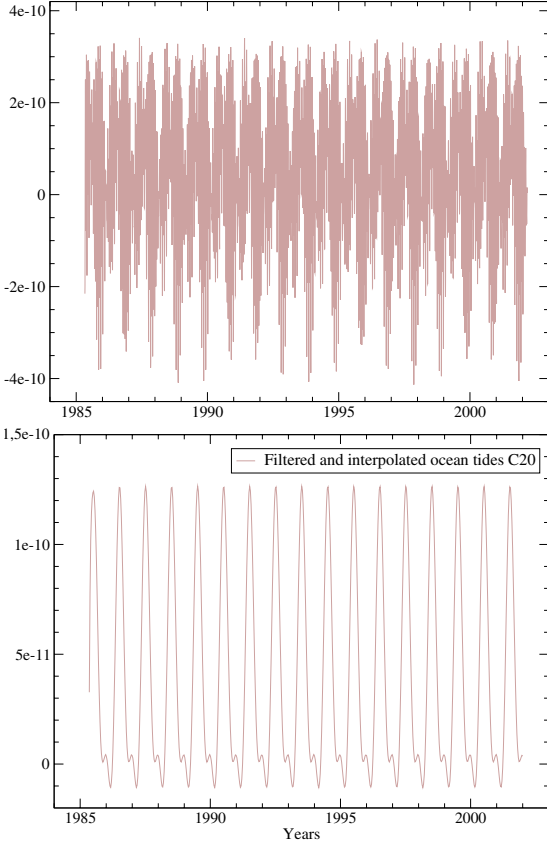
Fig. 5. Normalized oceanic ΔC_{20} (*top*: raw data, *bottom*: filtered data, where the high frequency signals have been removed): oceanic-tide-modelled part of the ΔC_{20} harmonic coefficient of the Earth gravity field; IERS Conventions 1996.

Fig. 6. Normalized solid tides ΔC_{20} (*top*: raw data, *bottom*: filtered data, where the high frequency signals have been removed): solid-Earth-tide-modelled part of the ΔC_{20} harmonic coefficient of the Earth gravity field; IERS Conventions 1996.

gravitational potential, we obtain the atmospheric pressure contribution to the $\Delta \bar{C}_{20}$ harmonic coefficient:

$$\Delta \bar{C}_{20\text{atm}}(t) = \frac{4\pi R_e^2 (1 + k_2')}{5Mg} \Delta \bar{C}_{20\text{ECMWF}}(t). \tag{23}$$

- The contribution of the oceanic tides (see Fig. 5) is modelled in the IERS Conventions 1996. The Earth responds to the dynamical effects of ocean tides, and the associated potential, limited to the degree 2 and order 0, is:
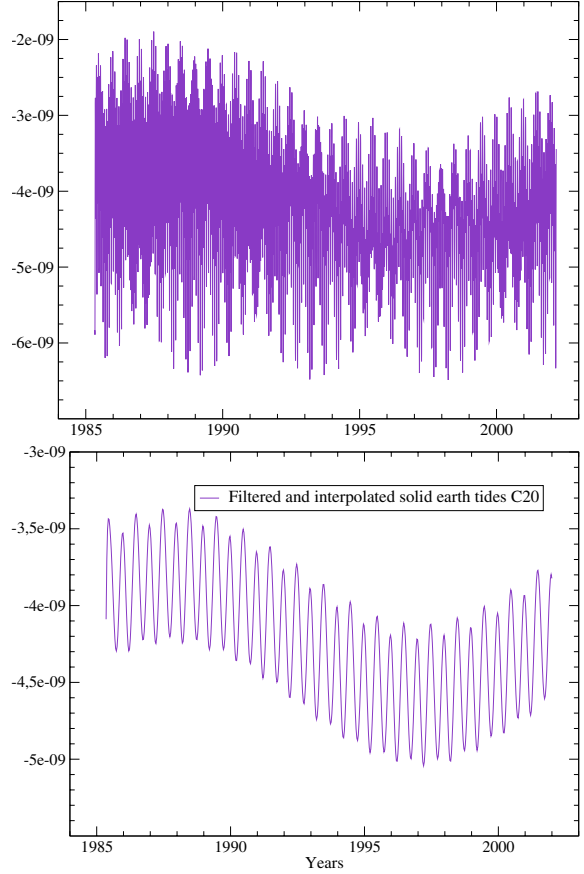
$$U_{\text{oc}} = 4\pi G R_e \rho_w \frac{1 + k_2'}{5} \left(\frac{R_e}{r}\right)^3 \bar{P}_{20}(\sin\phi)\,\alpha(t) \tag{24}$$

where we note α, depending on time, as:

$$\alpha = \sum_n \sum_+^- C_{n,2,0}^{\pm}\,\cos(\theta_n(t) + \chi_n) + S_{n,2,0}^{\pm}\,\sin(\theta_n(t) + \chi_n). \tag{25}$$

The sum over n corresponds to the Doodson development whose associated arguments are θ_n and χ_n. The parameter ρ_w (=1025 kg m^{-3}) is the mean density of sea water. Furthermore, $C_{n,2,0}^{\pm} = \hat{C}_{n,2,0}^{\pm} \sin(\epsilon_{n,2,0}^{\pm})$ and $S_{n,2,0}^{\pm} = \hat{C}_{n,2,0}^{\pm} \cos(\epsilon_{n,2,0}^{\pm})$, where $\hat{C}_{n,2,0}^{\pm}$ and $\epsilon_{n,2,0}^{\pm}$ are the normalized amplitude and phase of the harmonic model of the oceanic tides limited to degree 2 and order 0. Identifying Eq. (24) with the Earth gravitational potential gives the oceanic tide contribution to the $\Delta \bar{C}_{20}$ harmonic coefficient:

$$\Delta \bar{C}_{20\text{oc}}(t) = \frac{4\pi R_e^2 (1 + k_2')\rho_W}{5\,M}\,\alpha(t). \tag{26}$$

- The solid Earth tide contribution (see Fig. 6) is due to the gravitational effect of the Moon and the Sun on the Earth (IERS Conventions 1996). This force derives from a potential, developed in spherical harmonics, which limited to degree 2 and order 0 is:

$$U_{\text{soltid}} = G\,M\,\frac{R_e^2}{r^3}\,\bar{P}_{20}(\sin\phi)\,\bar{C}_{20\text{Moon+Sun}}(t) \tag{27}$$

where

$$\bar{C}_{20\text{Moon+Sun}}(t) = \frac{k_{20}\,R_e^3}{5\,M} \sum_{p=\text{moon}}^{\text{sun}} \left(\frac{m_p}{r_p^3}\,\bar{P}_{20}(\sin\phi_p)\right) \tag{28}$$

where $k_{20} = 0.3019$ is the nominal degree Love number for degree 2 and order 0, m_p the mass of the body p, and r_p the geocentric distance and ϕ_p the geocentric latitude at each moment of the body p. The Love number depends on the tidal frequencies acting on the Earth. Hence, the contribution to $\Delta \bar{C}_{20}$ from the long period tidal constituents of various frequencies ν must be corrected (see IERS Conventions 1996). Equation (27) corrected for the frequency dependence of the Love number, can be identified with the Earth gravitational potential. We obtain the Earth solid tide contribution to the $\Delta \bar{C}_{20}$ harmonic coefficient:

$$\Delta \bar{C}_{20\text{soltid}}(t) = \bar{C}_{20\text{Moon+Sun}} + \text{"frequency correction"}. \tag{29}$$
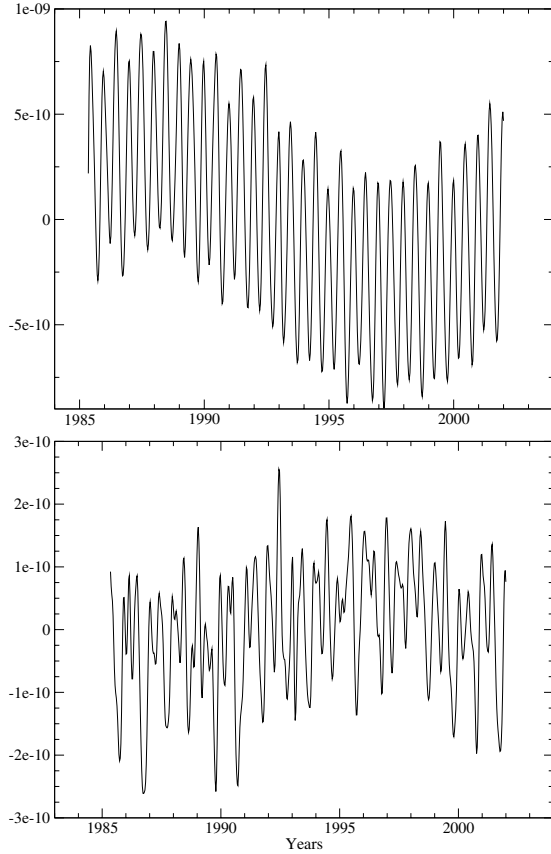
Fig. 7. Normalized total ΔC_{20}: top is the total series including atmospheric, oceanic tides and solid earth tides effects and the residuals; bottom is the total series without the solid earth tides effect.

This contribution comprises a constant part in the $\Delta \bar{C}_{20}$ solid Earth tide, which is called "permanent tide". We have estimated it and obtained: -4.215114×10^{-9} (the IERS Conventions value is -4.201×10^{-9}). We must remove it from our $\Delta \bar{C}_{20}$ data coming from solid Earth tides.

- Finally, we must consider a series including all the effects described before. Hence, we add them back to the residuals (Fig. 2), interpolating and filtering the data. Then we obtain the total series (Fig. 7).

4.3. Adjustments in ΔH data

Equation (11) allows us to transform the geodetic $\Delta \bar{C}_{20}$ temporal variations into the dynamical flattening variations ΔH. They can then be introduced into the precession Eq. (1), replacing H with $(H + \Delta H)$ (Eqs. (2)–(4) and (7)) and using the process already described in Sect. 2.3.

It is generally considered that VLBI observations of the Earth's orientation in space are not sensitive to the atmospheric and oceanic contributions to the variations in C_{20} (de Viron 2004). However the amplitudes of these effects have been evaluated in Table 11 for further discussion and in any case we can notice that they have a negligible effect on precession.

The analytical and semi-analytical approach to solving the precession-nutation equations provides polynomial developments of the ψ_A and ω_A quantities. The ΔH data are then considered as a linear expression plus Fourier terms with periods

Table 4. Summary of the constant parts for H and C_{20} (Constant part + Permanent tide) used in this study.

H_{MHB}	3.2737942×10^{-3}
$\bar{C}_{20}$	-4.841695×10^{-4}
J_2	1.0826358×10^{-3}
H^*	3.2671524×10^{-3}
H^* with geophysical constant parts	3.2671521×10^{-3}
H^{**}	3.2735556×10^{-3}

derived from a spectral analysis (18.6-yr, 9.3-yr, annual and semi-annual terms) (see Tables 4–7). Note that the phase angles used for adjusting the ΔH periodic terms are those of the corresponding nutation terms. This implies changes in the development of the equatorial precession angles (ψ_A, ω_A), which we describe in the next section.

For the residual contribution of ΔH, we will consider (i) an adjustment of a secular trend over the interval from 1985 to 1998 (see Table 6 and Eq. (30)), and (ii) an adjustment of a secular trend plus a 18.6-yr periodic term (see Table 5 and Eq. (31)), both added to the seasonal terms. The fit (i) of the secular trend gives:

$$\dot{H} \simeq -7.4 \times 10^{-9}/\mathrm{cy} \;\Leftrightarrow\; \dot{J}_2 \simeq -2.5 \times 10^{-9}/\mathrm{cy} \qquad (30)$$

and the fit of model (ii) gives:

$$\Delta H = \left(74 \times 10^{-11}\right) \times t + \left(20.9 \times 10^{-11}\right) \times \sin(\omega t)$$
$$+ \left(32.5 \times 10^{-11}\right) \times \cos(\omega t) \qquad (31)$$

with $\omega = 2\pi/0.186$.

We must recall that these adjustments have been made together with the fit of annual and semi-annual terms. In contrast, the higher frequency terms appearing in the ΔH data have been filtered and we therefore did not take into account other contributions, as for example the diurnal effects of the geophysical contributions in ΔH.

5. Effects of the ΔH contributions on the precession angles

On the basis of the models fitted to the time series of ΔH in the previous section, obtained with geodetic ΔC_{20} series, we investigate the influence of these geodetic data on the precession angle developments. First, we evaluate the effect of the secular trend considered in the $\Delta \bar{C}_{20}$ residual series. Second, we report on the influence of each geophysical contribution, on the influence of the residuals and on that of the total contribution. Finally we focus on the periodic effects resulting from the various ΔH contributions.

5.1. $\dot{J}_2$ influence

We have already mentioned that the $\dot{J}_2$ influence was taken into account in previous precession solutions (Williams 1994; Capitaine et al. 2003) (see Sect. 4.1). But depending on the

Table 5. Adjustment of periodic terms in the ΔH contributions, for the data span 1985−2002 for various ΔH geophysical sources (atmospheric $\Delta H_{\text{atm.}}$, oceanic tides $\Delta H_{\text{oc.}}$ and solid earth tides $\Delta H_{\text{soltid.}}$, as well as the residuals $\Delta H_{\text{res.}}$) – Units are in 10^{-10} rad.

| Period | $\Delta H_{\text{res.}}$ | | $\Delta H_{\text{atm.}}$ | | $\Delta H_{\text{oc.}}$ | | $\Delta H_{\text{soltid.}}$ | |
(in years)	sin	cos	sin	cos	sin	cos	sin	cos
1	2.17	−4.02	0.96	−1.66	−3.92	1.41	−4.64	0.89
0.5	−0.43	3.71			0.76	1.56	−0.34	28.04
18.6	2.09	3.25					−0.46	−26.29
9.3	−0.17	−1.65					−0.01	0.29

Table 6. Specific adjustment of the ΔH residual series ($\Delta H_{\text{res.}}$), from 1985 to 1998. The secular trend is considered as in Eq. (30) – Units are in 10^{-10} rad.

| Period | $\Delta H_{\text{res.}}$ | |
(in years)	sin	cos
1	2.57	−3.84
0.5	−0.50	3.80

Table 7. Adjustment of the total series of ΔH ($\Delta H_{\text{tot.}}$), from 1985 to 2002 – Units are in 10^{-10} rad.

| Period | $\Delta H_{\text{tot.}}$ | |
(in years)	sin	cos
1	−5.39	−3.39
0.5	0.07	33.67
18.6	0.92	−23.11
9.3	−0.08	−0.50

value adopted, the polynomial development of the ψ_A precession angle is different. Indeed, if we take $\dot{J}_2 = -2.5 \times 10^{-11}$/cy like in our study, or $\dot{J}_2 = -3 \times 10^{-11}$/cy like in Capitaine et al. (2003), the contribution in ψ_A varies by about 1.5 mas/cy^2 (see Table 8). So we must carefully take into account this J_2 rate. Furthermore, (i) we already noticed that such a secular trend has been recently discussed because of the change in this trend in 1998 (see Fig. 2); and (ii) the uncertainty in this secular trend, derived from space measurements of J_2, is significant. Therefore we can conclude that until there is a better determination of the J_2 rate, the accuracy of the precession expression is limited to about 1.5 mas/cy^2.

5.2. Precession

First, we can compare the polynomial part of our solution Geod04 for the precession angles, based on the constant part H_{MHB} of H and on its variable part provided by expression (31), with previous precession expressions (IAU2000 and P03) (see Table 9). The differences larger than one μas concern the ψ_A precession angle and more particularly its t^2 and t^3 terms. The differences (of 7 mas and 2 μas, respectively) with respect to P03 are due to considering or not considering the $\dot{J}_2$ effect. Actually, P03 includes a J_2 secular

trend, whereas Geod04 includes instead a 18.6-yr periodic term (see (3) in Table 9 or (2) in Table 10). Comparing Geod04 with the IAU2000 precession (which does not consider the J_2 rate) shows differences of 0.6 mas and 5 μas in the t^2 and t^3 terms, respectively. This results from the improved dynamical consistency of the Geod04 solution (based on the P03 precession equations) with respect to IAU2000. Note that such results regarding the t^2 and t^3 terms will not be affected if changes of the order of 1 mas/cy in the precession rate would occur in an updated P03 solution.

Second, we can evaluate the differences introduced in the ψ_A (and ω_A) polynomial development by the use of a constant part for H determined with the geodetic J_2 (as used in *Geod04-H** and *Geod04-H***) instead of the H_{astro} determined by VLBI and used in *Geod04*. Table 9 shows that the differences are very large, but it should be noted that using J_2 for deriving H suffers from the too large errors introduced by the mismodelled C/MR_{e}^2.

5.3. Periodic contributions

On the basis of the adjustments made in Sect. 4.3 for the different ΔH contributions, we estimate here the periodic effects appearing in the expressions of the precession angles. We can focus on the Fourier terms in the ψ_A precession angle, which are the most sensitive to the ΔH effects. The corresponding results are presented in Table 11.

- First, we note that the major effect is due to the 18.6-yr periodic term in the solid Earth tides (contribution number (3) of Table 11): about -2 μas and 120 μas in cosine and sine, respectively. The tidal annual and semi-annual effects are negligible as well as the atmospheric and oceanic effects (contributions number (4) and (5) of Table 11).

- Second, note that the ΔH variation strictly limited to its residual part, not modelled into the geodetic orbit restitution, introduces negligible Fourier terms into the ψ_A development. But we can note that the way the long term effect is considered in such data (i.e. either with a secular trend term (contribution number (1) of Table 11) or a 18.6-yr periodic term (contribution number (2) of Table 11)) is important. Modelling the long term variation in the geodetic residuals over the total data span as a 18.6-yr variation induces a term with an amplitude of 15 μas in the ψ_A development. But at present the ΔC_{20} data span is not long enough to allow us to discriminate between the two models.

Table 8. Influence of $\dot{J}_2$ on the polynomial development of ψ_A (more particularly on the t^2 and t^3 terms): (1) IAU2000 (Mathews et al. 2002); (2) P03 (Capitaine et al. 2003); and (3) Same computation as in P03 but with other $\dot{J}_2$ values. The J_2 secular trend estimation based on our C_{20} residuals series is: $\dot{J}_2 = -2.5 \times 10^{-9}$/cy.

	$\dot{J}_2$	t^2	t^3
(1) IAU2000	None	$-1''07259$	$-0''001147$
(2) P03	-3×10^{-9}/cy	$-1''079007$	$-0''001140$
		Differences wrt P03	
	0 /cy	-7.000 mas	2 μas
	-2×10^{-9}/cy	-2.871 mas	1 μas
(3)	-2.3×10^{-9}/cy	-1.954 mas	1 μas
	-2.5×10^{-9}/cy	-1.495 mas	1 μas

Table 9. Polynomial part of the ψ_A and ω_A developments (units in arcseconds): comparison of (1) IAU2000 (Mathews et al. 2002) – (2) P03 (Capitaine et al. 2003) – (3) Differences of Geod04 (this study) with respect to P03, considering all the contributions for ΔH (Table 7, ΔH_{tot}) – (4) Differences of Geod04 with respect to P03, obtained with a H constant part different from H_{MHB}, but not used in the following (see Table 3 for the H^* and H^{**} constant values).

Angle	Source		t^0	t	t^2	t^3
	(1) *IAU2000*			$5038''478750$	$-1''07259$	$-0''001147$
	(2) *P03*			$5038''481507$	$-1''079007$	$-0''001140$
				Differences wrt P03		
ψ_A	(3) Geod04	H_{MHB}		$0''$	-7 mas	2 μas
	(4) Geod04	H^*		$\simeq 10''23$	-9.177 mas	-3 μas
		H^{**}		$\simeq 0''37$	-7.079 mas	2 μas
	(1) *IAU2000*		$84381''448$	$-0''025240$	$0''05127$	$-0''00772$
	(2) *P03*		$84381''406$	$-0''025754$	$0''051262$	$-0''007725$
				Differences wrt P03 in μas		
ω_A	(3) Geod04	H_{MHB}	0	0	0	0
	(4) Geod04	H^*	0	0	104	-35
		H^{**}	0	0	3	-1

Finally, we can conclude that the geodetic determination of the total variable C_{20} (contribution number (6) of Table 11) introduces Fourier terms into the ψ_A precession angle development, mainly a 18.6-yr periodic one, of the order of 4 μas and 105 μas in cosine and sine, respectively.

6. Discussion

This study was based on new considerations: the use of a geodetic determination of the variable geopotential to investigate its influence on the developments of the precession angles. The major effect on the precession is due to the J_2 secular trend which implies an acceleration of the ψ_A precession angle. But for the moment, the available time span for J_2 satellite series is not as long as we need to determine a reliable $\dot{J}_2$ value. The J_2 secular trend estimation based on our C_{20} residuals

series from 1985 to 1998 is: $\dot{J}_2 = -2.5 \times 10^{-9}$/cy. The accuracy of the precession expression is limited to about 1.5 mas/cy^2 due to the uncertainty in this J_2 rate value.

Then, we can notice that the main periodic effect is due to the 18.6-yr periodic term in ΔC_{20} due to solid Earth tides. But we must say that computing the ΔC_{20} with satellite positioning observations requires making some assumptions on the geophysical contributions to ΔC_{20}, for instance from atmospheric pressure, and oceanic or solid Earth tides. Actually, models are used, but they are not perfect and we may have some errors. So the ΔC_{20} residuals obtained may be affected by these errors, which is why the total ΔC_{20} contributions (residuals observed + models assumed) constitute a better series to evaluate the effects on the precession angles. This introduces Fourier terms into the ψ_A development (4 μas and 105 μas in cosine and sine respectively; see Table 11) that we should

Table 10. Polynomial part of the ψ_A development (units in arcseconds) for various ΔH sources used in our study, with respect to P03: comparison of (1) P03 (Capitaine et al. 2003) – (2) Difference between P03 and Geod04 (i.e. the effect of the total ΔH) – (3) Difference between P03 and the effect of the ΔH residuals.

Angle	Source		t	t^2	t^3
	(1) *P03*		5038$.\!\!''$481507	$-1.\!\!''$079007	$-0.\!\!''$001140
				Differences wrt P03 in μas	
ψ_A	(2) Geod04 total contributions		0	-7000	2
	(3) Geod04 residuals $\Big\{$	1985$-$1998	0	-1495	1
		1985$-$2002	0	-7000	2

Table 11. Fourier part of the ψ_A development, depending on the contribution considered for the ΔH periodic effect (units in μas).

				Periodic contribution for the t^0 term of ψ_A	
				μas	
				cos	sin
	(1)	Residuals (1985$-$1998)	Annual	-1	-1
			Semi-annual	$-$	1
	(2)	Residuals (1985$-$2002)	18.6-yr	10	-15
			9.3-yr	$-$	4
			Annual	-1	-1
			Semi-annual	$-$	1
ΔH periodic contributions	(3)	Solid tides	18.6-yr	-2	120
			9.3-yr	$-$	-1
			Annual	1	$-$
			Semi-annual	$-$	3
	(4)	Ocean tides	Annual	1	$-$
			Semi-annual	$-$	$-$
	(5)	Atmosphere	Annual	$-$	$-$
	(6)	Geod04 total contributions	18.6-yr	4	105
			9.3-yr	$-$	1
			Annual	1	-1
			Semi-annual	$-$	4

compare to the MHB2000-nutations. Indeed, the different terms of the total ΔH (or ΔC_{20}) contributions have same periods as the ($\Delta\psi$, $\Delta\epsilon$) nutations. This implies that there is some coupling between the observed ΔH effects and the nutations, which may not have been included in the MHB2000-nutations.

In the future, we will be able to compare the J_2 data with geophysical models and data, in order to have better ideas on the different contributions and on the secular trend. We will also be able to proceed to numerical study of this problem, and to implement a refined and more realistic Earth model.

References

Biancale, R., Lemoine, J.-M., Loyer, S., Marty, J.-C., & Perosanz, F. 2002, private communication of the C_{20} data

Bianco, G., Devoti, R., Fermi, M., et al. 1998, Planet. Space Sci., 46, 1633

Bretagnon, P., Rocher, P., & Simon, J.-L. 1997, A&A, 319, 305

Bretagnon, P., Fienga, A., & Simon, J.-L. 2003, A&A, 400, 785

Capitaine, N., Wallace, P. T., & Chapront, J. 2003, A&A, 412, 567

Capitaine, N., Wallace, P. T., & Chapront, J. 2004, A&A, 421, 365

Cazenave, A., Gegout, P., Ferhat, G., & Biancale, R. 1995, IAG Symp., ed. R. H. Rapp, A. A. Cazenave, & R. S. Nerem, 116, 141

Chao, B., & Au, A. Y. 1991, J. Geophys. Res., 96, 6569

Chapront, J. 2003, Notice, Paris Observatory (January 2003)

Cox, C. M., & Chao, B. 2002, Science, 297, 831

Dehant, V., & Capitaine, N. 1997, Celest. Mech. Dyn. Astr., 65, 439

Dehant, V., Arias, F., Bizouard, C., et al. 1999, Celest. Mech. Dyn. Astr., 72, 245

de Viron, O. 2004, private communication

Dickey, J. O., Marcus, S. L., De Viron, O., & Fukumori, I. 1975, Science, 298

Farrell, W. E. 1972, Rev. Geophys. Space Phys., 10, 761

Fukushima, T. 2003, Astr. J., 126, 494

Gegout, P., & Cazenave, A. 1993, Geophys. Res. Let., 18, 1739

Kinoshita, H. 1977, Celest. Mech., 15, 277

Lambeck, K. 1988, Geophysical geodesy: The Slow Deformations of the Earth, Oxford Science Publications

Lambert, S., & Capitaine, N. 2004, A&A, 428, 255

Lieske, J. H., Lederle, T., Fricke, W., & Morando, B. 1977, A&A, 58, 1

Mathews, P. M., Herring, T. A., & Buffett, B. A. 2002, J. Geophys. Res., 107, B4

McCarthy, D. D. 1996, IERS Conventions, 21, Observatoire de Paris, Paris

Morrison, L., & Stephenson, R. 1997, Contemporary Physics, 38, 13

Nerem, R. S., Chao, B. F., Au, A. Y., et al. 1993, Geophys. Res. Let., 20, 595

Souchay, J., & Kinoshita, H. 1996, A&A, 312, 1017

Souchay, J., & Folgueira, M. 1999, Earth, Moon and Planets, 81, 201

Williams, J. G. 1994, AJ, 108 (2), 711

Yoder, C. F., Williams, J. G., Dickey, J. O., et al. 1983, Nature, 303, 757